Monsoonal Influence on Typhoon Morakot (2009). Part II: Numerical Study

JIA LIANG AND LIGUANG WU

Key Laboratory of Meteorological Disaster of Ministry of Education, Nanjing University of Information Science and Technology, Nanjing, China

XUYANG GE

International Pacific Research Center, SOEST, University of Hawaii at Manoa, Honolulu, Hawaii

CHUN-CHIEH WU

Department of Atmospheric Sciences, National Taiwan University, Taipei, Taiwan

(Manuscript received 12 November 2010, in final form 30 March 2011)

ABSTRACT

In the second part of this study, numerical experiments are conducted to investigate the influences of multi-time-scale monsoonal flows on the track change of Typhoon Morakot (2009). While the control simulation captures the slowing and northward deflections in the vicinity of Taiwan Island, the highly asymmetric rainfall structure, and the associated rainfall pattern, sensitivity experiments suggest that the westward movement prior to the landfall on Taiwan and the subsequent northward shifts in the vicinity of Taiwan were closely associated with the interaction between Morakot and multi-time-scale monsoonal flows.

Prior to the landfall on Taiwan, Morakot moved westward directly toward Taiwan because of a synoptic wave train–like pattern, which consisted of Goni over mainland China, Morakot, and a cyclone over the western North Pacific with an anticyclone to the west of Morakot. Numerical simulation suggests that strong northerly winds between Morakot and the anticyclone reduced the northward steering component associated with the low-frequency flow prior to the landfall. Numerical experiments confirm that the northward track shifts that occurred in the vicinity of Taiwan Island were a result of the coalescences of Morakot with a quasi-biweekly oscillation (QBW)-scale gyre prior to the landfall on Taiwan and a Madden–Julian oscillation (MJO)-scale gyre in the Taiwan Strait. The simulation of Morakot and the associated sensitivity experiments agree with the previous barotropic study that the interaction between tropical cyclones and low-frequency monsoon gyres can cause sudden changes in tropical cyclone tracks.

1. Introduction

In Part I of this study (Wu et al. 2011a, hereafter Part I) the influences of multi-time-scale monsoonal flows on the track change and precipitation structure of Typhoon Morakot (2009) were examined observationally. Embedded in multi-time-scale monsoon flows, Typhoon Morakot generally moved westward prior to its landfall on Taiwan and underwent a coalescence process first with a cyclonic gyre on the quasi-biweekly oscillation (QBW) time scale and then with a cyclonic gyre on the Madden–Julian oscillation (MJO)-time scale. Observational analysis in Part I suggested that the multi-time-scale monsoonal flows played an important role in the associated record-breaking rainfall. The synoptic-scale southwesterly winds on the southeastern side of the typhoon were enhanced through coalescences with the QBW-scale and MJO-scale cyclonic gyres and thus reduced the westward movement of the typhoon, leading to an unusually long residence time and a northwestward track shift in the vicinity of Taiwan. Meanwhile, the coalescences of Morakot with the low-frequency gyres maintained the primary rainband associated in southern Taiwan although the typhoon moved northwestward across Taiwan and into the Taiwan Strait.

Although Carr and Elsberry (1995) suggested that many sudden track changes over the western North Pacific are

Corresponding author address: Dr. Liguang Wu, Pacific Typhoon Research Center, Key Laboratory of Meteorological Disaster of Ministry of Education, Nanjing University of Information Science and Technology, Nanjing, Jiangsu 210044, China.
E-mail: liguang@nuist.edu.cn

DOI: 10.1175/2011JAS3731.1

associated with the coalescence of typhoons with monsoon gyres, the mechanism was investigated only in idealized numerical experiments with a barotropic vorticity equation model. Together with the sudden track changes discussed in Wu et al. (2011b), the first part of this study provided more observational evidence to show that this mechanism was responsible for the observed track changes of Morakot in the vicinity of Taiwan Island. In the second part of this study, the influences of multi-time-scale monsoonal flows on the track change and rainfall structure of Morakot are further examined by conducting a series of numerical experiments with the Weather Research and Forecasting model (WRF). Our focus is placed mainly on the individual contributions of the monsoonal flows on the MJO, QBW, and synoptic time scales to the track change of Morakot.

It has been long known that the island effect can also deflect tropical cyclone tracks (Brand and Blelloch 1973; Tuleya and Kurihara 1978; Chang 1982; Tuleya et al. 1984; Bender et al. 1985). In particular, the topographic effect of Taiwan Island was confirmed numerically through simulating typhoons that made landfall on the island (e.g., Yeh and Elsberry 1993a,b; Wu and Kuo 1999; Wu 2001; Wu et al. 2002; Chiao and Lin 2003; Chen and Yau 2003; Lin et al. 2005; Chien et al. 2008; Lee et al. 2008; Jian and Wu 2008; Yang et al. 2008; Wu et al. 2009). Since the track changes of Morakot occurred in the vicinity of Taiwan Island, numerical experiments are also conducted to demonstrate how Taiwan Island affected the track of Morakot.

2. Model and experiment design

The numerical experiments in this study are conducted with the Advanced Research WRF (ARW-WRF) model. The model configuration is the same as used that in Ge et al. (2010). The numerical simulations include three two-way interactive domains with horizontal resolutions of 27, 9, and 3 km (Fig. 1). The outermost and middle domains cover the regions of 0.8°S–46.4°N, 98.3°–151.7°E and 12.4°–36.4°N, 111.6°–138.4°E, respectively. The innermost domain is designed to move with the tropical cyclone (TC). The model has 28 levels in the vertical with a top of 50 hPa. The WRF single-moment (WSM) three-class simple ice microphysics scheme (Dudhia 1989) and the Kain–Fritch convective scheme (Kain and Fritch 1993) are used in the outermost domain, and the WSM five-class microphysics scheme (Hong et al. 2004) is used in the middle and innermost domains with no convective parameterization. The Yonsei University PBL scheme (Noh et al. 2003), the Dudhia shortwave parameterization (Dudhia 1989), and the Rapid Radiative Transfer Model (RRTM) longwave parameterization (Mlawer et al. 1997) are used for the radiation calculation in all of the three model domains.

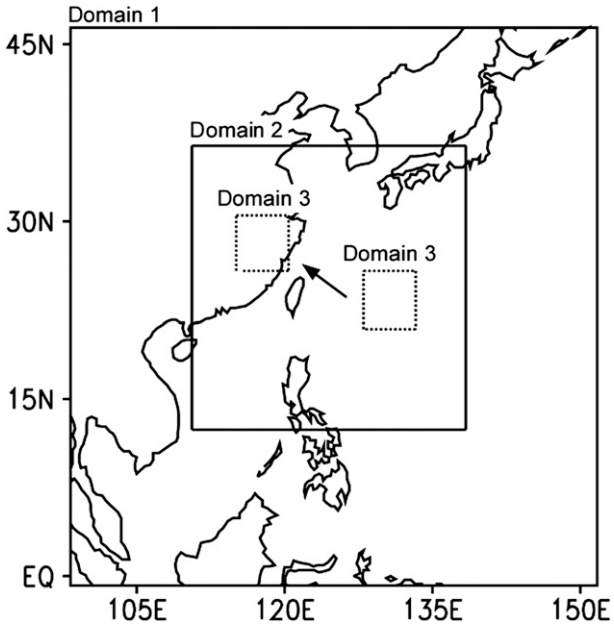

FIG. 1. Triple-nested domains used in the ARW-WRF simulations with the innermost domain (dashed) moving with Typhoon Morakot.

The National Centers for Environmental Prediction (NCEP) Final (FNL) Operational Global Analysis data on 1.0° × 1.0° grids at every 6 h are used to initialize the ARW-WRF model. The sea surface temperature (SST) is updated every 6 h. Because of the relatively low resolution of the FNL analyses, a TC initialization scheme is used for the model initial fields, which was described in Ge et al. (2010). An initial vortex with the minimum sea level pressure (MSLP) of 970 hPa, a radius of maximum wind of 100 km, and a size of 1000 km (where vortex wind speed becomes zero) is inserted into the environmental field derived from the FNL data (Fig. 2a). All of the numerical simulations cover a 108-h period from 1200 UTC 5 August to 0000 UTC 10 August 2009.

Six numerical experiments are carried out in this study (Table 1). In the control run (CTL), the realistic Taiwan topography and unfiltered initial fields are used in the model. Ge et al. (2010) designed terrain sensitivity experiments to examine the topographic effect of Taiwan Island on the record-breaking rainfall of Morakot in southern Taiwan. In their study the topography over Taiwan was set to be 100 m if the elevation was higher than the height. In this study, this experiment (T100) is rerun. To examine the influence of the surface property of Taiwan Island, a numerical experiment (OCEAN) is conducted by replacing Taiwan Island with ocean.

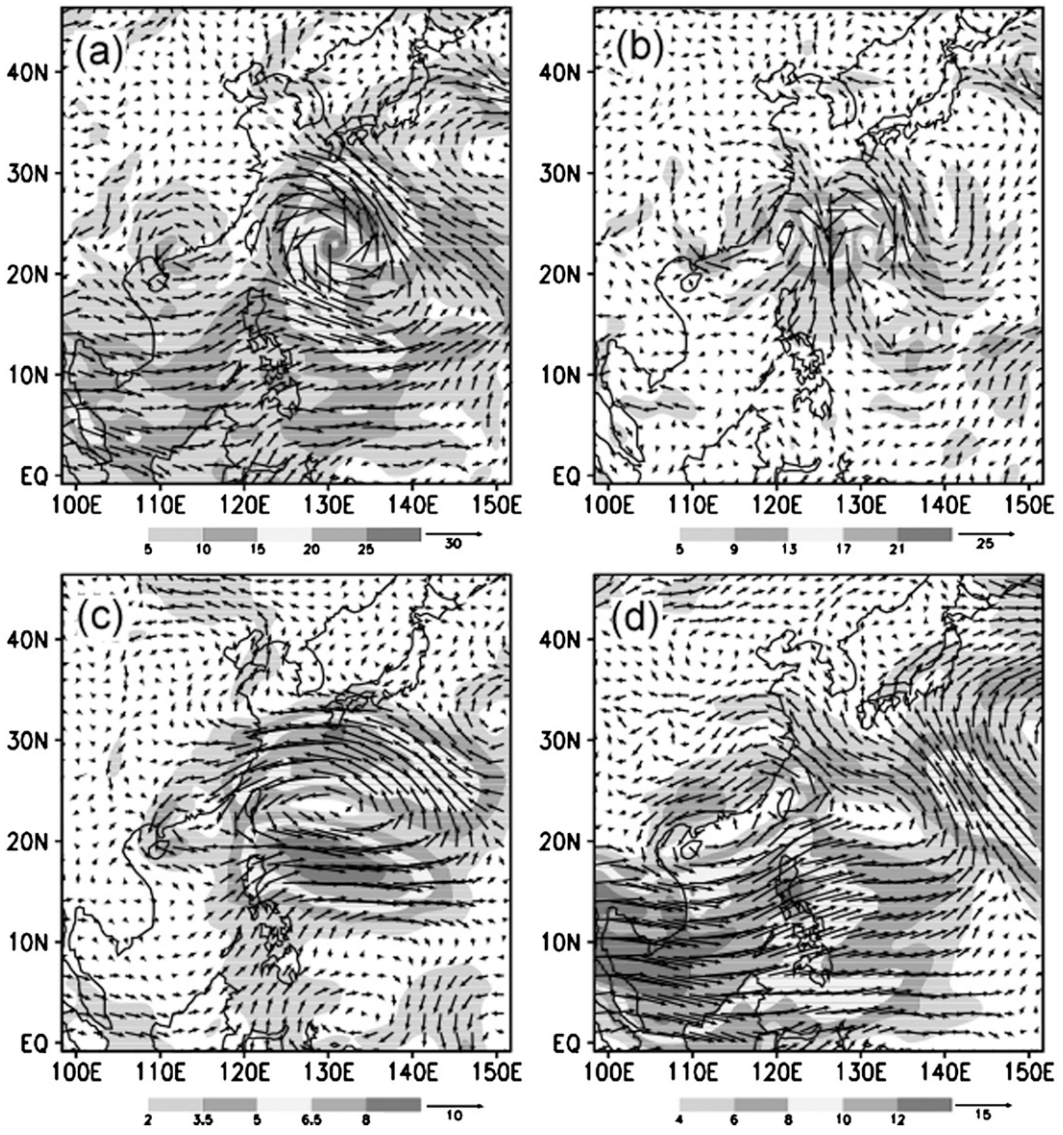

FIG. 2. (a) The unfiltered initial wind field at 700 hPa at 1200 UTC 5 Aug 2009 and the corresponding components on the (b) synoptic scale, (c) QBW scale, and (d) MJO scale with the shading indicating wind speeds (m s^{-1}). A bogus vortex that is not shown here is inserted into the initial conditions in the simulations.

The FNL-derived initial wind field associated with Morakot contains three components (Fig. 2). In this study, the Lanczos filter is used at each grid point to separate 20-day low-pass (hereafter MJO time scale) flows, 10–20-day bandpass (hereafter QBW time scale) flows, and synoptic-scale flows that are the difference between the unfiltered flows and the flows from a 10-day low-pass filter. The filter is also used for separate other

TABLE 1. Description of experiments for Typhoon Morakot.

Experiment	Description
CTL	Control run with the realistic Taiwan topography and unfiltered initial fields within a bogus.
T100	As in CTL, but the topography over Taiwan Island is set to 100 m if the elevation is higher than the value.
OCEAN	As in CTL, but replacing the Taiwan topography with ocean.
NO-QBW	As in CTL, but without QBW-scale flows in the model initial fields.
NO-SYN	As in CTL, but without the synoptic-scale flows in the model initial fields.
ONLY-MJO	As in CTL, but only MJO-scale flows (without QBW-scale and synoptic-scale flows) in the model initial fields.

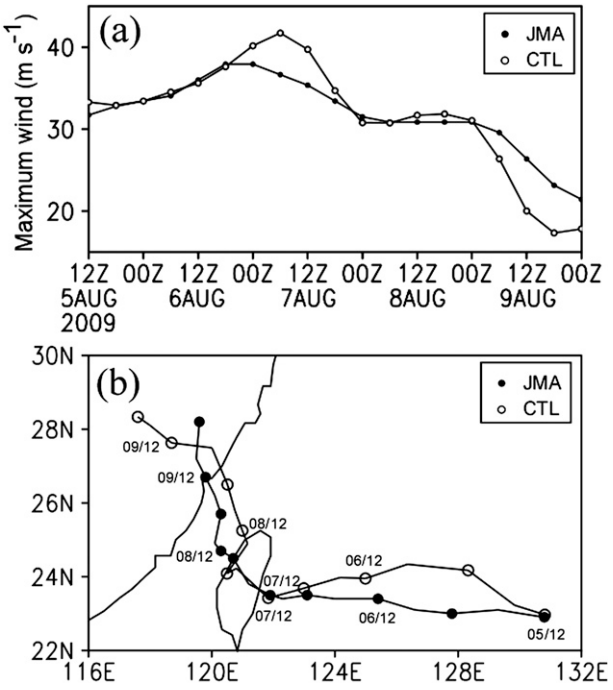

FIG. 3. The observed and simulated (a) intensity and (b) track of Typhoon Morakot from 1200 UTC 5 Aug to 0000 UTC 10 Aug 2009. The marks are at 12-h intervals.

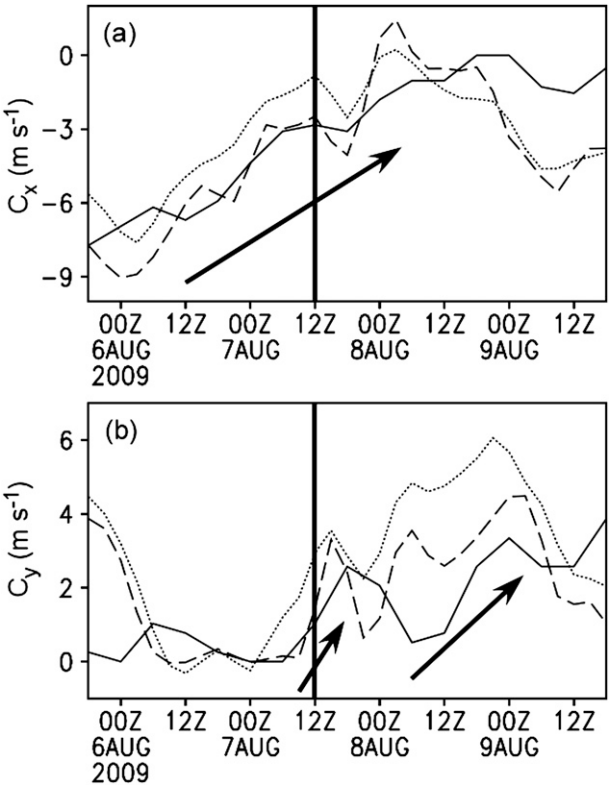

FIG. 4. Time series of (a) zonal speed C_x (m s^{-1}) and (b) meridional speed C_y (m s^{-1}) of observed (solid) and simulated translation speeds (dashed) and the speed of the steering flow (dotted) in CTL. The vertical lines indicate the landfall time and the arrows show the trends in speeds.

variables used in the initial and boundary conditions. An anticyclone on the synoptic time scale was located to the west of Morakot with strong northerly flows between the anticyclone and Morakot (Fig. 2b). A QBW-scale cyclonic gyre was located at 23°N, 130°E at 1200 UTC 5 August (Fig. 2c), which was embedded in a large MJO-scale monsoon gyre off the eastern coast of China with a trough extending southeast over the western North Pacific (Fig. 2d).

Three experiments are conducted to examine the individual influences of multi-time-scale monsoonal flows on Morakot. In the first two experiments (NO-QBW and NO-SYN), the QBW-scale and synoptic-scale components are removed from the model initial fields, respectively. In the third experiment (ONLY-MJO), both the QBW-scale and the synoptic-scale components are removed from the model initial fields. In other words, the initial conditions in ONLY-MJO contain the MJO-scale fields and the inserted symmetric vortex. Note that the corresponding components are also removed from the lateral boundary conditions.

3. Simulation results

a. The simulated Morakot in the control experiment

In this study, the simulated TC center is defined as that which maximizes the symmetric tangential wind (Wu et al. 2006). To determine the center, a variational approach is used to locate the TC center until the maximum azimuthal mean tangential wind speed is obtained. Figure 3 shows the simulated intensity and track in CTL during the period of 1200 UTC 5 August–0000 UTC 10 August, compared to the observed ones. The intensity evolution in CTL is very close to that of the Japan Meteorological Agency (JMA) best-track data. The simulated Morakot attains its peak intensity of about 42 m s^{-1} at 0600 UTC 7 August, 4 m s^{-1} stronger than the observed. The peak intensity appears about 6 h earlier than the observation, several hours before the typhoon makes landfall on Taiwan. Like the observation, the simulated Morakot weakens rapidly after its first landfall over Taiwan and second landfall over mainland China.

In general, the CTL simulation captures well the movement of Morakot during the period from 1200 UTC 5 August to 0000 UTC 10 August (Fig. 3b). The simulated TC initially moves northwestward, leading to a cyclonic turn prior to its landfall on Taiwan, whereas the observed track directly headed to Taiwan Island. At 1200 UTC 7 August, the center of the simulated TC is

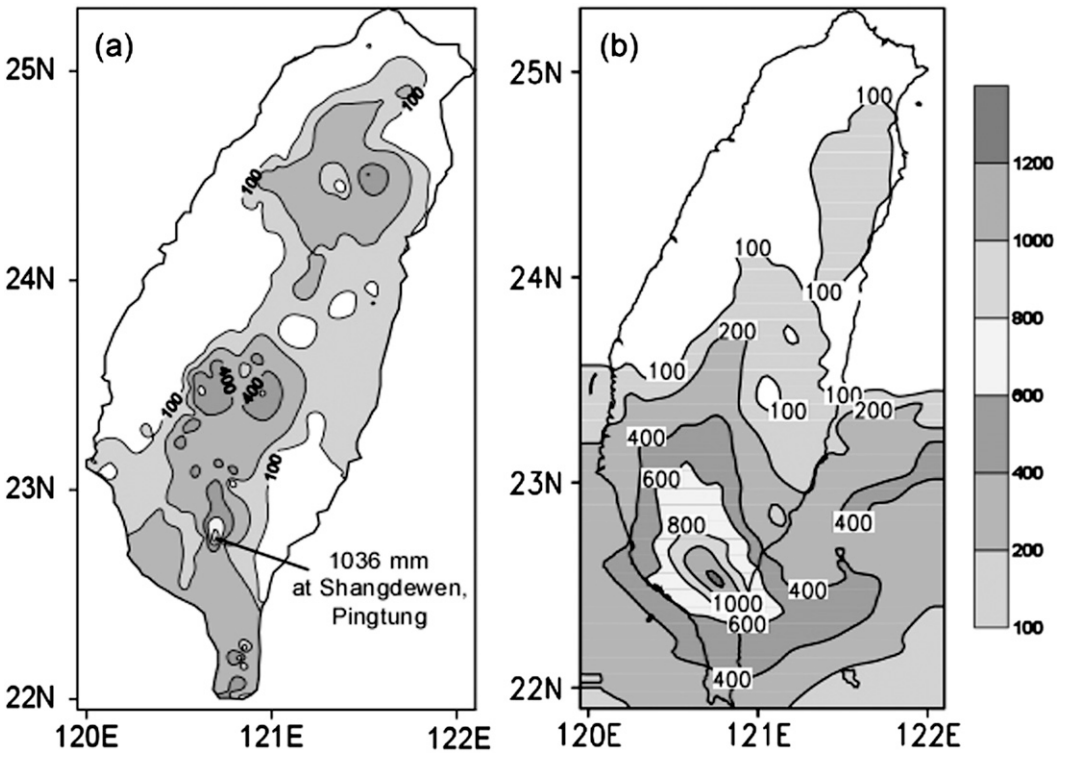

FIG. 5. The accumulated rainfall (mm) from (a) the Central Weather Bureau of Taiwan and (b) the 3-km grid simulation in CTL from 0300 UTC 7 Aug to 0300 UTC 8 Aug 2009.

nearly the same as the observed. The simulated TC takes 9 h to move northwestward across Taiwan Island. Over the island, the simulated track agrees well with the observed. Around 0000 UTC 8 August, the simulated TC takes a more northward track over the Taiwan Strait than the observed track. After making landfall over China mainland, the simulated TC makes a west-northwestward turn that did not occur in the observation. Despite the differences between the simulated and observed tracks, the CTL experiment simulated well the important features of the observed track of Morakot, including the landfall time and location and the northward deflections prior to its landfall over Taiwan and the Taiwan Strait.

The CTL experiment also simulates well the observed deceleration of the translation speed in the vicinity of Taiwan Island (Fig. 4). Since 0900 UTC 6 August, the westward component persistently decreases and it is about 3.0 m s^{-1} prior to the landfall over Taiwan. The westward movement slightly increases and then decreases again when the TC moves over Taiwan Island. This generally agrees with the observed zonal movement of Morakot. The simulated northward component decreases significantly during the first 12 h and the TC generally moves westward with a very small meridional component in the next 12 h. The northward component starts to increase just prior to the landfall, in good agreement with the observation (Fig. 4b). Because of the decreasing westward and increasing northward speeds, the simulated TC turns northwestward prior to Morakot's landfall over Taiwan Island. The second increase in the northward component occurs around 0000 UTC 8 August, about 6 h earlier than the observation, when the simulated TC is over the western coast of the island. Note that the simulated change of the translation speed is consistent with that of the steering flow calculated in the way described in Part I.

Because of the movement of the innermost domain, we can only compare the simulated 24-h accumulated rainfall with the observation during the period from 0300 UTC 7 August to 0300 UTC 8 August, while Morakot made landfall on and crossed Taiwan Island (Fig. 5). The simulated maximum rainfall of about 1200 mm is larger than the observed maximum rainfall of 1036 mm at the Shangdewen Station, Pingtung County. Additional simulations were conducted with Lin et al. (2005) and Goddard microphysics scheme respectively, where the maximum rainfall is much less than that in CTL (not shown). Since the focus of this study is not on the model physics intercomparison, the factors leading to the different rainfall in different moisture schemes are not

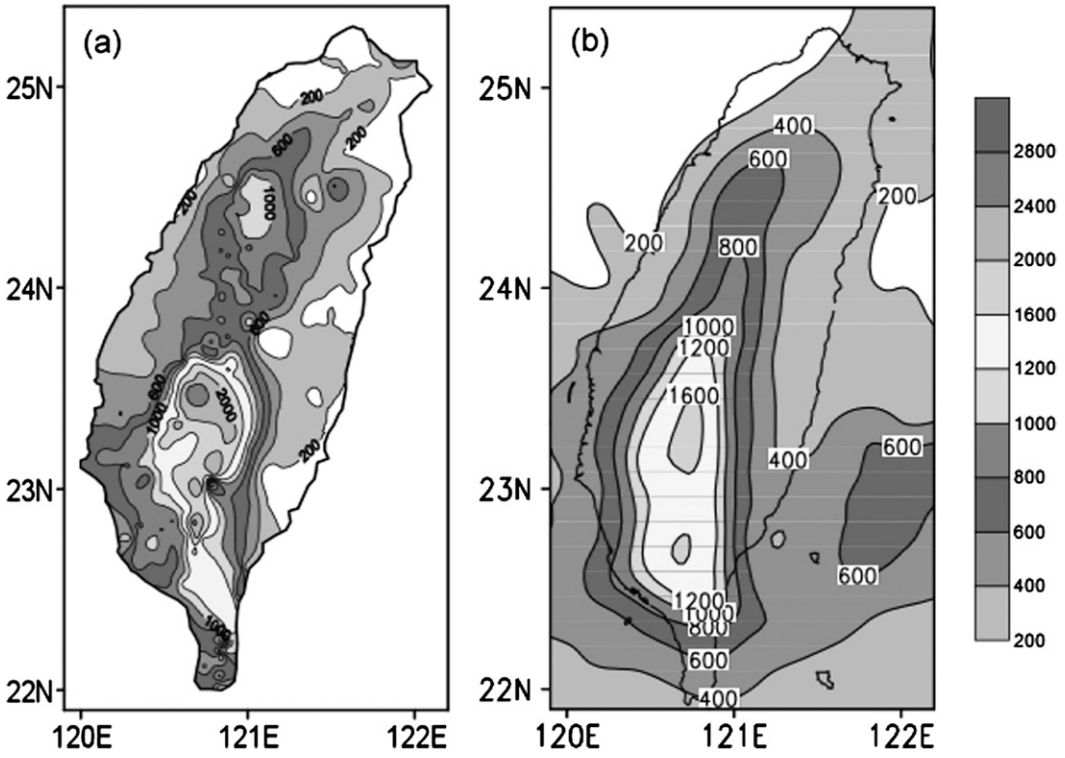

FIG. 6. The accumulated rainfall (mm) from (a) the observation of the Central Weather Bureau of Taiwan and (b) the simulation with 9-km grids in CTL from 1200 UTC 5 Aug to 0000 UTC 10 Aug 2009.

explored here. In addition, the spatial distribution of the simulated rainfall compares well with the observed, in particular the extreme rainfall in southern Taiwan. We also examine the spatial distribution of the simulated rainfall over the whole simulation period in the 9-km domain and find that simulated rainfall distribution is also in good agreement with the observation, although the maximum rainfall in the southern Taiwan is smaller than the observed due to the coarse resolution (Fig. 6).

As pointed out in the first part of this study, the convective activity associated with Morakot was highly asymmetric, mainly occurring on the southern side of the typhoon. The important feature is also well simulated in the CTL experiment. Figure 7 shows the simulated radar reflectivity of the innermost domain and 700-hPa winds fields of the outer coarse domain. At 1200 UTC 6 August (Fig. 7a), in addition to a nearly closed eyewall, a large area of deep convection can be found in the southwestern periphery of the typhoon. The closed eyewall disappears and the major convection occurs to the south of the typhoon center when the simulated Morakot approaches and makes landfall on Taiwan (Fig. 7b). As the typhoon moves into the Taiwan Strait (Fig. 7c), the main convective area is over southern Taiwan, 200–300 km away from the typhoon center. This is very similar to the observation that was examined in Part I. We can see that the CTL experiment well reproduces the observed convective asymmetry associated with Morakot.

In association with the high convective asymmetry, the maximum wind over 25 m s^{-1} mainly appears to the west and north of the typhoon center at 1200 UTC 6 August (Fig. 7d), together with relatively strong westerly winds (~20 m s^{-1}) over the Philippine Sea. On 7 August (Fig. 7e), the southwesterly winds are enhanced along the southern periphery of Typhoon Morakot with the area of strong southwesterly winds extending about 1000 km to the south and southeast of the typhoon center. The strong southwesterly winds extend farther southwestward into the South China and form a comma-shaped pattern on 8 August (Fig. 7f). Since the enhanced southwesterly winds do not shift northward with the movement of Morakot, the primary rainfall expands outward with time as the typhoon center moves northwestward after its landfall on Taiwan (Figs. 7a–c). In general, the evolution of the simulated southwesterly winds is consistent with the observation discussed in Part I.

b. *Influence of Taiwan Island*

The effect of Taiwan topography on Morakot is examined through the terrain sensitivity experiments including

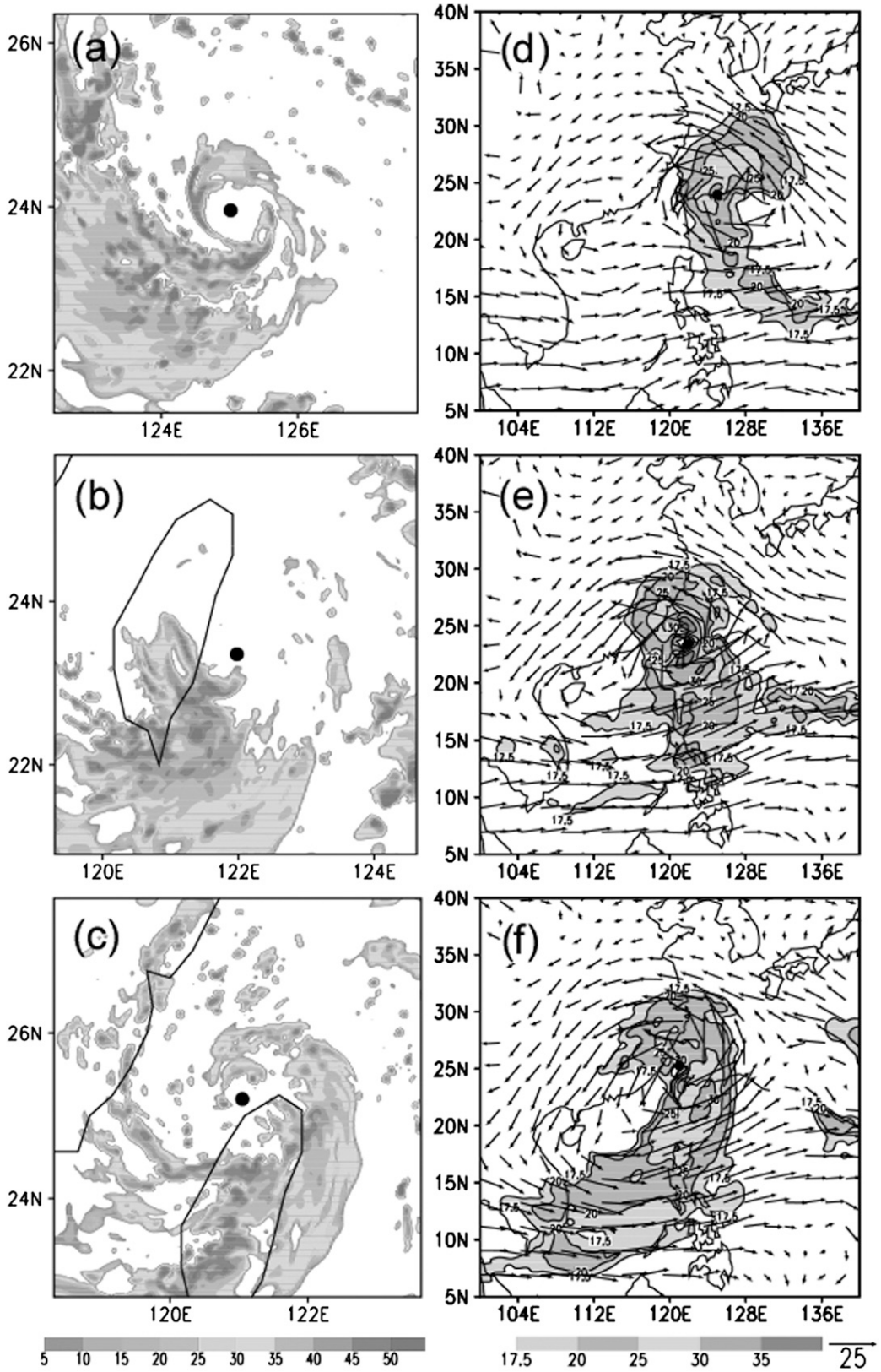

FIG. 7. (a)–(c) The simulated radar reflectivity (dBZ) in the innermost domain and (d)–(f) the simulated 700-hPa wind field (m s^{-1}) in the 27-km domain, for (a),(d) 1200 UTC 6 Aug, (b),(e) 1200 UTC 7 Aug, and (c),(f) 1200 UTC 8 Aug 2009. The typhoon center is indicated with black dots.

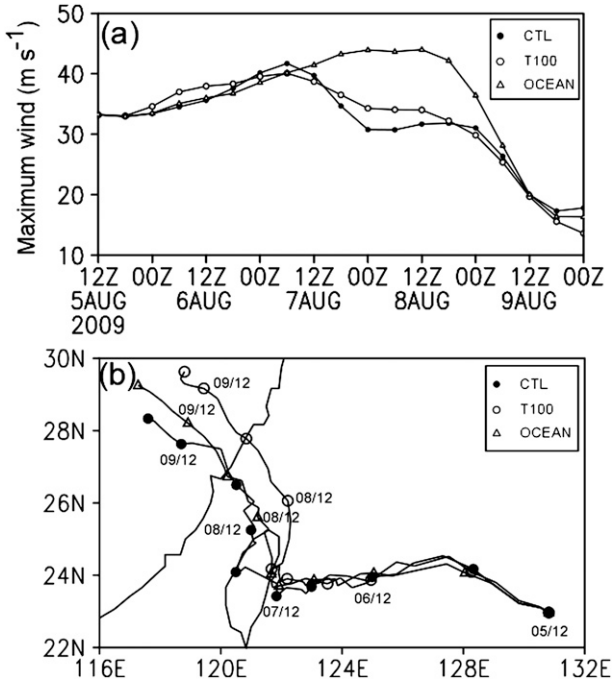

FIG. 8. The simulated (a) intensity and (b) track of Typhoon Morakot from 1200 UTC 5 Aug to 0000 UTC 10 Aug 2009. The marks are at 12-h intervals.

T100 and OCEAN. Figure 8 compares the simulated tracks and intensities in T100 and OCEAN with those in CTL during the period from 1200 UTC 5 August to 0000 UTC 10 August. As expected, the TC intensities in both terrain experiments are different from that in CTL, while the three simulations show a similar evolution in intensity prior to 7 August. As suggested by Ge et al. (2010), the lower the terrain height of Taiwan Island, the stronger the intensity of Morakot after landfall.

Both of the simulated tracks in T100 and OCEAN do not deviate significantly from that in CTL. As shown in Fig. 8b, during the first 30 h the simulated Morakot takes a cyclonic path similar to that in CTL. In the two experiments a more abrupt northward turn occurs before the TC makes landfall over Taiwan around 1200 UTC 7 August. In T100, the simulated typhoon approaches Taiwan Island and then suddenly turns northeastward off the eastern coast of northern Taiwan. The simulated TC does not make landfall over Taiwan and makes its first landfall on mainland China with the landfall location about 100 km to the north of that in CTL. In OCEAN, the simulated typhoon crosses northern Taiwan after a northward turn around 1200 UTC 7 August and then shows a track nearly identical to that in CTL over Taiwan Strait. Although Taiwan Island affects the track, it is clear that the sudden northward deflection of Morakot is not directly a result of the influence of the island.

However, as suggested by Ge et al. (2010), the influence of Taiwan Island on the rainfall associated with Morakot is clear. Figure 9 shows the simulated rainfall during the whole 108-h simulation period in the 9-km domain. While the maximum rainfall over 1600 mm is observed in CTL, the simulated rainfall center moves eastward to the eastern coast in OCEAN and over the ocean in T100, respectively. The spatial rainfall distribution in the 3-km domain in T100 and OCEAN shows the same variations (not shown). The different rainfall distributions may be associated with the simulated track differences. Hong et al. (2010) found that the combined low-frequency and typhoon flows, which converged and lifted by the Central Mountain Range, play an important role in the record-breaking rainfall associated with Morakot.

c. Influence of multi-time-scale monsoon flows

1) SYNOPTIC TIME-SCALE FLOWS

The influence of multi-time-scale monsoon flows on Morakot's track is examined by comparing experiments NO-SYN, NO-QBW, and ONLY-MJO with CTL. Figure 10 displays the simulated intensity and track in these experiments from 1200 UTC 5 August to 0000 UTC 10 August, suggesting the significant influence of multi-time-scale monsoon flows. In NO-SYN, the TC reaches its peak intensity around 0000 UTC 6 August (Fig. 10a), when it moves very slowly in low-frequency gyres (Figs. 2c,d). Under the influence of the steering flow associated with the low-frequency gyres, the TC first moves northeastward, suddenly turns northwestward at 0900 UTC 6 August, and then takes a northwestward track by 1200 UTC 7 August. During this period, the TC continues to weaken and maintains merely tropical storm intensity. An abrupt northward shift occurs around 1200 UTC 7 August, and the TC generally moves northward after the sudden turn. The simulated TC track is very similar to the cases discussed by Carr and Elsberry (1995). They found that sudden poleward track changes occur when a TC is embedded in a monsoon gyre. The NO-SYN experiment suggests that synoptic time-scale flows played an important role in the westward movement before Morakot made landfall over Taiwan.

Figure 11 shows the observed evolution of the 500-hPa synoptic time-scale winds. An anticyclone formed over the ocean to the east of the Philippines around 0600 UTC 2 August, which can be seen near the Philippines at 0000 UTC 4 August (Fig. 11a). At this time Tropical Storm Goni was located to its west. A remarkable feature is the nearly zonal synoptic wave train–like pattern (Figs. 11a–c), including Goni over Guangdong Province of

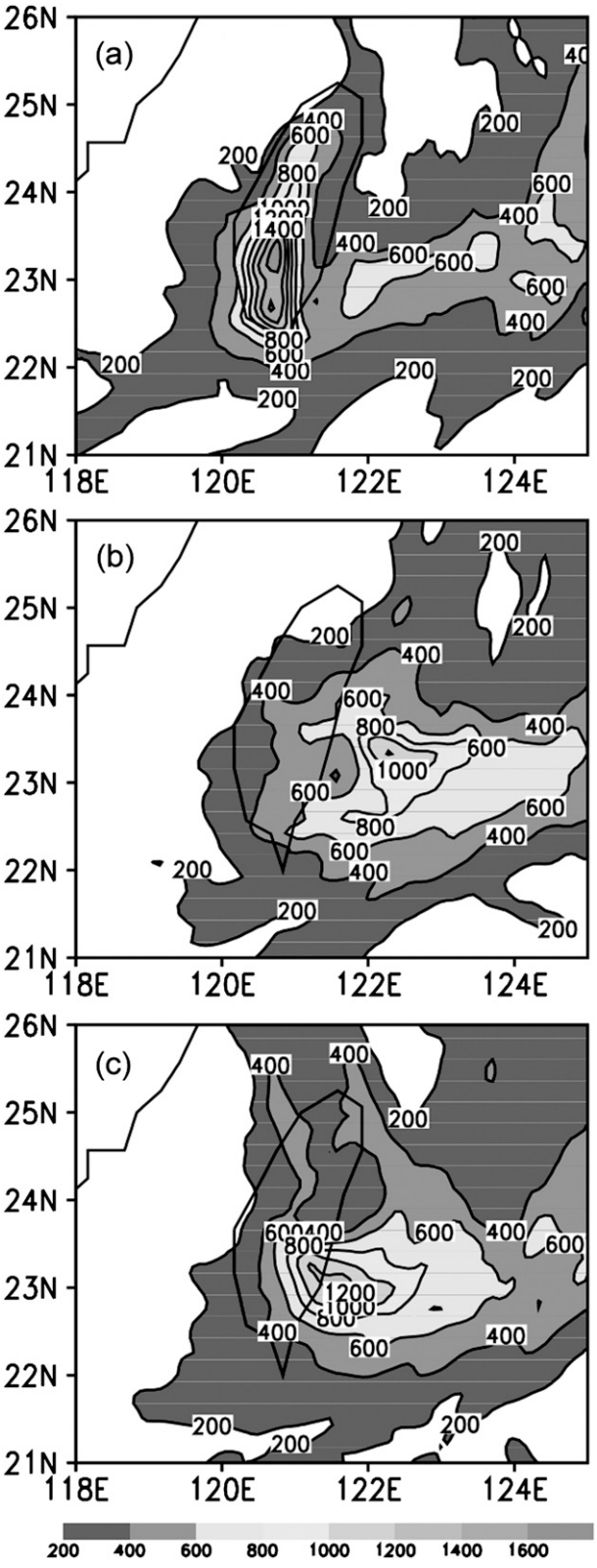

FIG. 9. The accumulated rainfall (mm) simulated in the 9-km domain in (a) CTL, (b) T100, and (c) OCEAN from 1200 UTC 5 Aug to 0000 UTC 10 Aug 2009.

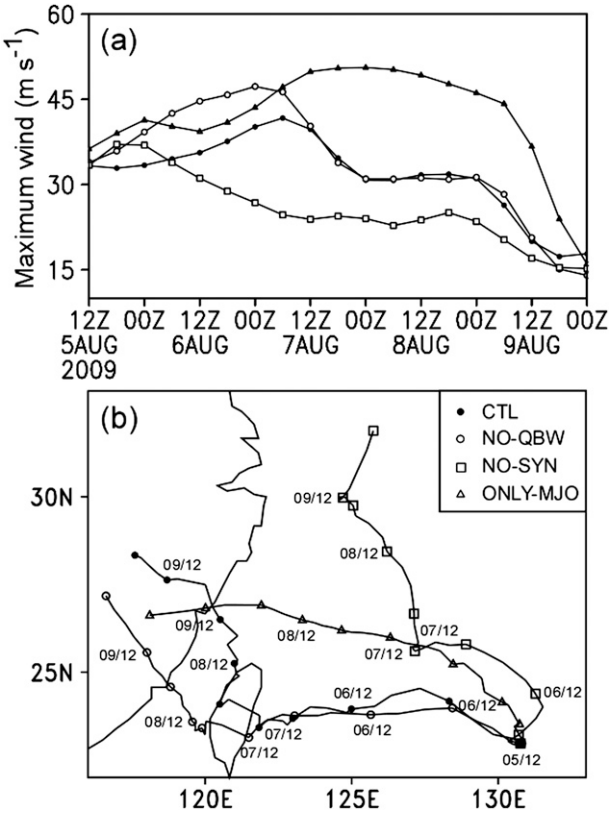

FIG. 10. The simulated (a) intensity and (b) track of Typhoon Morakot from 1200 UTC 5 Aug to 0000 UTC 10 Aug 2009. The marks are at 12-h intervals.

China, Morakot (indicated with the closed dot), and a cyclonic vortex (C) over the western North Pacific, which developed into Tropical Storm Etau later. The synoptic wave train–like pattern was maintained until 0000 UTC 7 August and strong northerly winds between the anticyclone A1 and Morakot reduced the northward component of the steering flow associated with the low-frequency gyres (Figs. 2c,d). The initial formation of A1 may be due to the Rossby energy dispersion associated with Goni.

Figure 12 shows the 700-hPa winds associated with the simulated TC in NO-SYN. At 0000 UTC 6 August (Fig. 12a), the simulated TC is embedded in a large monsoon gyre about 200 km to the southeast of the gyre center. It is initially steered by the southwesterly flow associated with the monsoon gyre. It turns northwestward at 0900 UTC 6 August when it is located to the east of the gyre center (Fig. 12b). On early 7 August (Fig. 12c), the TC becomes concentric with the monsoon gyre and a weak anticyclonic circulation can be found to the southeast of the simulated TC. As suggested by Carr and Elsberry (1995), the anticyclone results from the Rossby wave energy dispersion associated with the monsoon

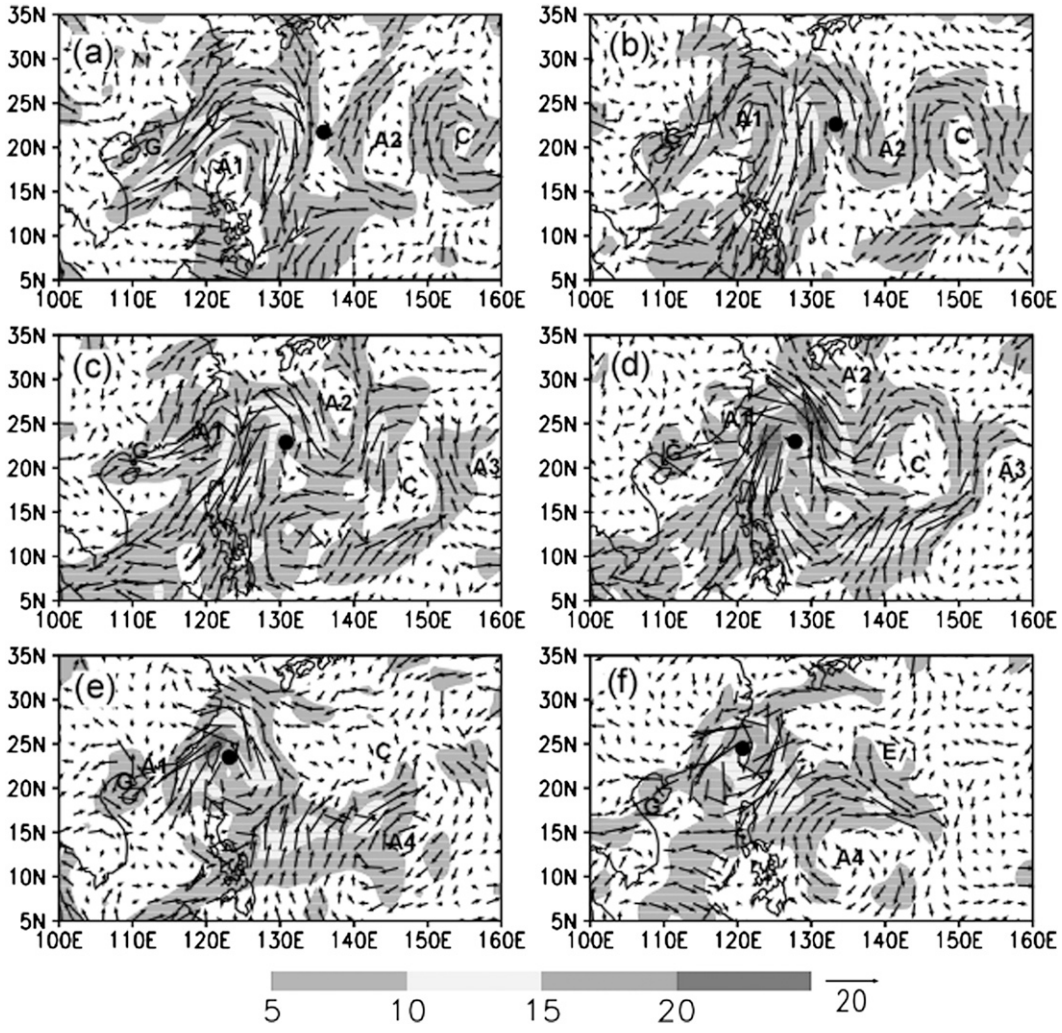

FIG. 11. The 500-hPa 10-day high-pass filtered winds (m s^{-1}) at (a) 0000 UTC 4 Aug, (b) 0000 UTC 5 Aug, (c) 1200 UTC 5 Aug, (d) 0000 UTC 6 Aug, (e) 0000 UTC 7 Aug, and (f) 0000 UTC 8 Aug 2009, respectively. The black dot and letters G and E indicate the centers of Typhoon Morakot, Tropical Storm Goni, and Tropical Storm Etau, respectively.

gyre. As the TC coalesces with the monsoon gyre, the enhanced southwesterly surge provides a northeastward steering flow, leading to a northeastward deflection around 1200 UTC 9 August (Fig. 12d).

2) LOW-FREQUENCY FLOWS

In NO-QBW, the intensity evolution of the TC is similar to that in CTL, except with a stronger intensity by 1200 UTC 7 August (Fig. 10a). The TC takes a cyclonic path similar to that in CTL before its landfall (Fig. 10b). On early 6 August, it turns slightly to the south of the track in CTL and makes landfall on Taiwan around 1200 UTC 7 August, when the simulated TC reaches its peak intensity. Then the TC moves slightly northwestward and takes about 9 h to cross the island with an overland track nearly parallel to that in CTL. Compared to the TC track in CTL, the simulated TC in NO-QBW does not make a northward deflection off the eastern coast of Taiwan.

Figure 13 shows the 700-hPa winds associated with the simulated TC in NO-QBW. At 1200 UTC 6 August (Fig. 13a), strong winds (>25 m s^{-1}) appear on the northern side of the TC without relatively strong southwesterly winds over the Philippine Sea, which occur in CTL (Fig. 7a). As the TC moves westward toward Taiwan, the associated winds in its southern periphery gradually increase, leading to a relatively symmetric wind structure (Fig. 13b). By 0000 UTC 8 August the comma-shaped area of gale force winds (>17.5 m s^{-1}) that occurs in CTL does not appear in this experiment (Fig. 13c).

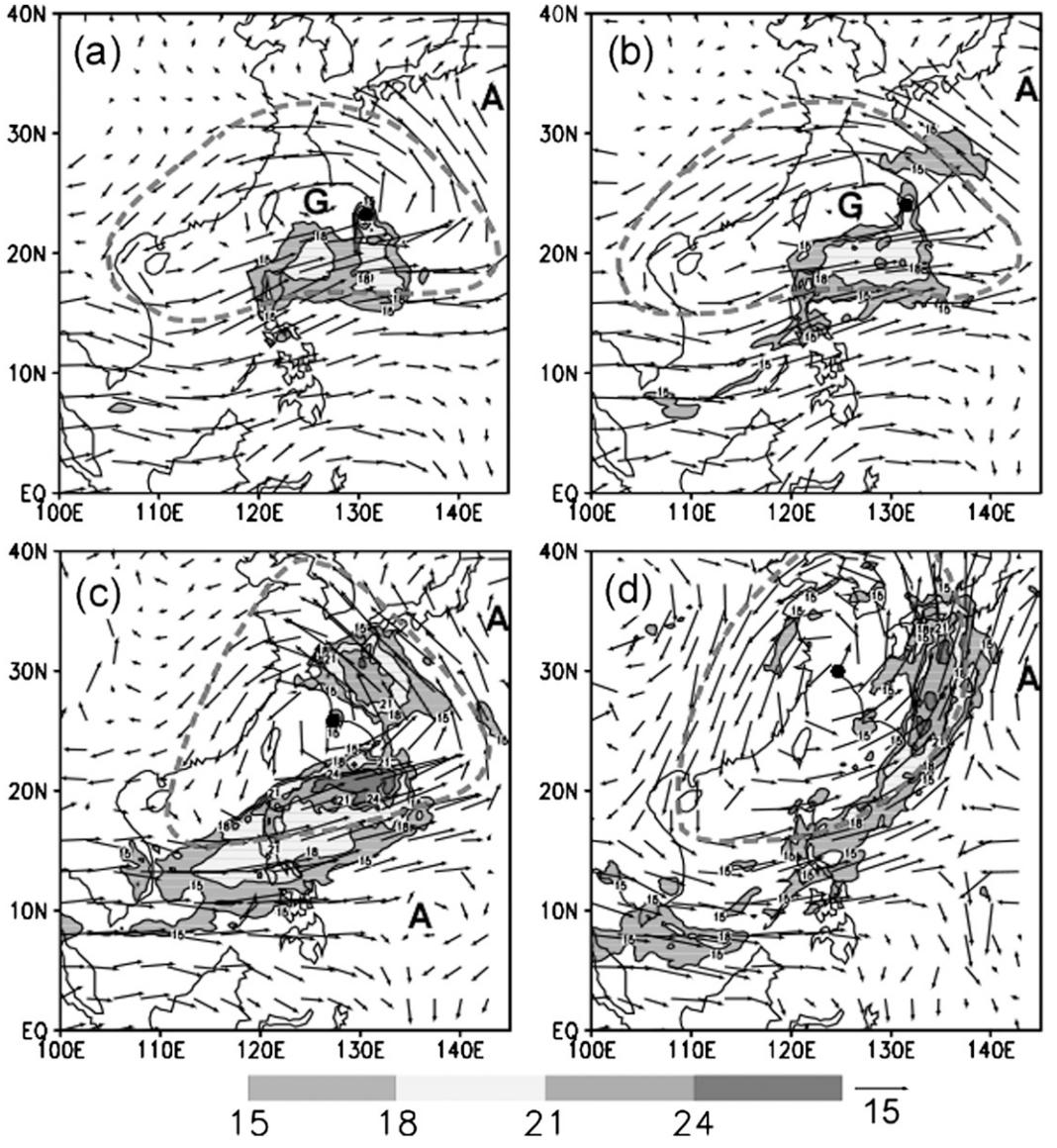

FIG. 12. The simulated 700-hPa wind fields (m s^{-1}) in the 27-km domain on 700 hPa in NO-SYN at (a) 0000 UTC 6 Aug, (b) 0900 UTC 6 Aug, (c) 1800 UTC 7 Aug, and (d) 1200 UTC 9 Aug 2009. The gray dashed lines roughly outline the monsoon gyre.

As a result, because of the absence of the strong northward steering flow that results from the interaction between the TC and the QBW-scale gyre in CTL, the northward deflection that occurs around 1200 UTC 7 August in CTL is not observed in NO-QBW. During the next 12 h (Fig. 13d), the southwesterly wind in the southern periphery enhances sharply and extends to the South China Sea. The enhanced southwesterly winds result from the interaction between the simulated TC and the MJO-scale gyre and turn the TC northward around 1200 UTC 8 August (Fig. 2d). The TC approaches the MJO-scale gyre center, leading to enhancement of the southwesterly winds, which steer the TC northward.

In ONLY-MJO the TC intensifies slightly during the first 12 h and then intensifies again after 1200 UTC 6 August (Fig. 10a). It attains its peak intensity of 48 m s^{-1} at 0000 UTC 8 August because of the absence of the influence of Taiwan Island. The simulated TC takes a rather smooth west-northwestward track and makes its first landfall on China mainland around 1200 UTC 9 August. Because of the slow-varying monsoon trough, as shown in Fig. 2d, the TC is generally steered by the southeasterly flows associated with the monsoon

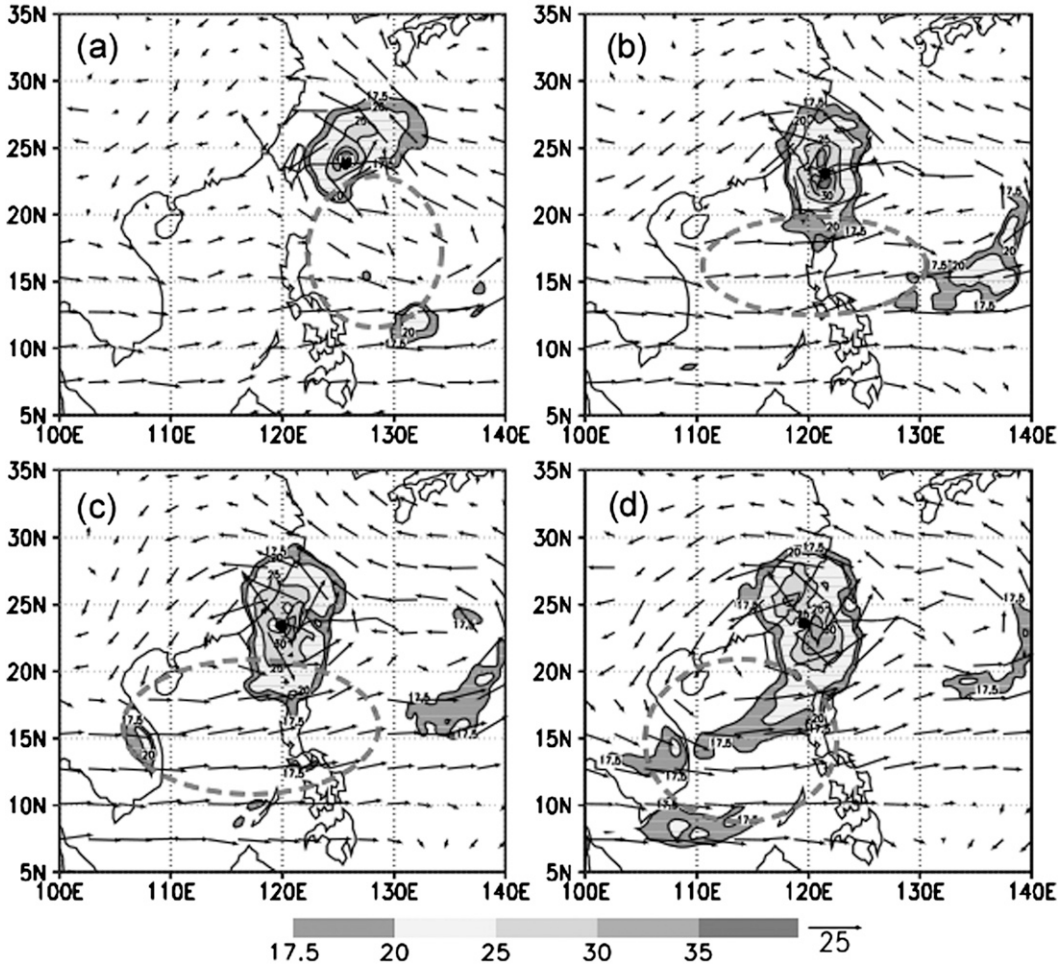

FIG. 13. As in Fig. 12, but for NO-QBW at (a) 1200 UTC 6 Aug, (b) 1200 UTC 7 Aug, (c) 0000 UTC 8 Aug, and (d) 1200 UTC 8 Aug 2009. The gray dashed lines roughly outline the areas of enhanced southwesterly winds in Fig. 7.

trough. This experiment also confirms the important roles of the various time-scale flows in the movement of Morakot.

4. Summary

In the second part of this study, the influences of multi-time-scale monsoon flows on the track change and rainfall structure of Typhoon Morakot are investigated through numerical experiments with the ARW-WRF model, with a focus on how the multi-time-scale monsoon flows affect the track change of Typhoon Morakot. The effect of the Taiwan terrain is also examined in this study.

The control experiment can reproduce well the intensity evolution, track changes, and rainfall distribution of Typhoon Morakot. In particular, the model can capture the northward deflections and slowing down when Morakot crosses Taiwan Island and the Taiwan Strait. In agreement with the observed, the highly asymmetric structure of the typhoon is reasonably simulated with the maximum accumulated rainfall in southern Taiwan. In agreement with Ge et al. (2010), the sudden northward deflections of Morakot's track is not directly due to the influence of the island, while the terrain effect of Taiwan Island is remarkable on the rainfall associated with Morakot. The numerical experiments conducted with the initial fields on the combination of different time scales indicate that the synoptic-scale, QBW-scale, and MJO-scale monsoonal flows play an important role in the record-breaking rainfall event associated with Morakot.

It is found that prior to the landfall on Taiwan the westward movement is closely associated with a nearly zonal synoptic-scale wave train–like pattern, which consists of Goni over Guangdong Province, Morakot, and a cyclone over the northern West Pacific. The strong northerly winds between the anticyclone between Goni and Morakot reduced the northward steering component associated with the low-frequency gyres,

leading to Morakot's westward movement directly toward Taiwan.

The track change of Morakot in the vicinity of Taiwan is closely associated with its interaction with the low-frequency monsoonal flows. When Morakot approached to Taiwan, it coalesced with a QBW-scale gyre. As a result, the southwesterly winds were enhanced in the southern periphery of Morakot, reducing its westward movement and leading to the first northward deflection in the track of the typhoon. As Morakot moved into the Taiwan Strait, it merged with a large MJO-scale gyre and made the second northward shift in its track. The numerical experiments confirm that the coalescence of a TC with a monsoon gyre can lead to sudden changes in TC tracks, as suggested by Carr and Elsberry (1995). This study agrees with Ko and Hsu (2006, 2009) that the intraseasonal oscillation (ISO) flows are associated with recurving TC tracks.

Typhoon Morakot formed in a large-scale monsoon trough over the western North Pacific. Its cyclonic circulation contained significant components of monsoon flows on the MJO and QBW time scales when it merged with the low-frequency gyres. The numerical experiments confirm that the coalescence of Morakot with low-frequency monsoon gyres enhanced the synoptic-scale southwesterly winds on the southern side of Morakot and reduced its westward movement, leading to an unusually long residence time of the typhoon in the vicinity of Taiwan. In addition, as suggested by Hong et al. (2010), the overlaid southwesterly winds maintained the primary rainfall area in southern Taiwan as the typhoon center moved northwestward after its landfall on Taiwan. In agreement with Ge et al. (2010), it is found that the extreme rainfall event was closely associated with the lifting effect of Taiwan's terrain.

Acknowledgments. This research was jointly supported by the Typhoon Research Project (2009CB421503) of the National Basic Research Program of China, the National Science Foundation of China (NSFC Grant 40875038), the Social Commonweal Research Program of the Ministry of Science and Technology of the People's Republic of China (GYHY200806009), and the Research Innovation Program for college graduates of Jiangsu Province (CX10B_290Z). Chun-Chieh Wu was supported by Grant NSC97-2111-M-002-016-MY3.

REFERENCES

Bender, M. A., R. E. Tuleya, and Y. Kurihara, 1985: A numerical study of the effect of a mountain range on a landfalling tropical cyclone. *Mon. Wea. Rev.,* **113,** 567–582.

Brand, S., and J. W. Blelloch, 1973: Changes in the characteristics of typhoons crossing the Philippines. *J. Appl. Meteor.,* **12,** 104–109.

Carr, L. E., and R. L. Elsberry, 1995: Monsoonal interactions leading to sudden tropical cyclone track changes. *Mon. Wea. Rev.,* **123,** 265–290.

Chang, S. W.-J., 1982: The orographic effects induced by an island mountain range on propagating tropical cyclones. *Mon. Wea. Rev.,* **110,** 1255–1270.

Chen, Y., and M. K. Yau, 2003: Asymmetric structures in a simulated landfalling hurricane. *J. Atmos. Sci.,* **60,** 2294–2312.

Chiao, S., and Y.-L. Lin, 2003: Numerical modeling of an orographically enhanced precipitation event associated with Tropical Storm Rachel over Taiwan. *Wea. Forecasting,* **18,** 325–344.

Chien, F.-C., Y.-C. Liu, and C.-S. Lee, 2008: Heavy rainfall and southwesterly flow after the leaving of Typhoon Mindulle (2004) from Taiwan. *J. Meteor. Soc. Japan,* **86,** 17–41.

Dudhia, J., 1989: Numerical study of convection observed during the winter monsoon experiment using a mesoscale two-dimensional model. *J. Atmos. Sci.,* **46,** 3077–3107.

Ge, X., T. Li, S. Zhang, and M. Peng, 2010: What causes the extremely heavy rainfall in Taiwanduring Typhoon Morakot (2009)? *Atmos. Sci. Lett.,* **11,** 46–50, doi:10.1002/asl.255.

Hong, C.-C., M.-Y. Lee, H.-H. Hsu, and J.-L. Kuo, 2010: Role of submonthly disturbance and 40–50 day ISO on the extreme rainfall event associated with Typhoon Morakot (2009) in southern Taiwan. *Geophys. Res. Lett.,* **37,** L08805, doi:10.1029/2010GL042761.

Hong, S.-Y., J. Dudhia, and S.-H. Chen, 2004: A revised approach to ice microphysical processes for the bulk parameterization of cloud and precipitation. *Mon. Wea. Rev.,* **132,** 103–120.

Jian, G.-J., and C.-C. Wu, 2008: A numerical study of the track deflection of Supertyphoon Haitang (2005) prior to its landfall in Taiwan. *Mon. Wea. Rev.,* **136,** 598–615.

Kain, J. S., and J. M. Fritch, 1993: Convective parameterization for mesoscale models: The Kain–Fritch scheme. *The Representation of Cumulus Convection in Numerical Models, Meteor. Monogr.,* Amer. Meteor. Soc., No. 46, 165–170.

Ko, K.-C., and H.-H. Hsu, 2006: Sub-monthly circulation features associated with tropical cyclone tracks over the East Asian monsoon area during July–August season. *J. Meteor. Soc. Japan,* **84,** 871–889.

——, and ——, 2009: ISO modulation on the submonthly wave pattern and the recurving tropical cyclones in the tropical western North Pacific. *J. Climate,* **22,** 582–599.

Lee, C.-S., Y.-C. Liu, and F.-C. Chien, 2008: The secondary low and heavy rainfall associated with Typhoon Mindulle (2004). *Mon. Wea. Rev.,* **136,** 1260–1283.

Lin, Y.-L., S.-Y. Chen, C. M. Hill, and C.-Y. Huang, 2005: Control parameters for the influence of a mesoscale mountain range on cyclone track continuity and deflection. *J. Atmos. Sci.,* **62,** 1849–1866.

Mlawer, E. J., S. J. Taubman, P. D. Brown, M. J. Iacono, and S. A. Clough, 1997: Radiative transfer for inhomogeneous atmosphere: RRTM, a validated correlated-*k* model for the longwave. *J. Geophys. Res.,* **102** (D14), 16 663–16 682.

Noh, Y., W. G. Cheon, S.-Y. Hong, and S. Raasch, 2003: Improvement of the *K*-profile model for the planetary boundary layer based on large-eddy simulation data. *Bound.-Layer Meteor.,* **107,** 401–427.

Tuleya, R. E., and Y. Kurihara, 1978: A numerical simulation of the landfall of tropical cyclones. *J. Atmos. Sci.,* **35,** 242–257.

——, M. A. Bender, and Y. Kurihara, 1984: A simulation study of the landfall of tropical cyclones using a movable nested-mesh model. *Mon. Wea. Rev.,* **112,** 124–136.

Wu, C.-C., 2001: Numerical simulation of Typhoon Gladys (1994) and its interaction with Taiwan terrain using the GFDL hurricane model. *Mon. Wea. Rev.,* **129,** 1533–1549.

——, and Y.-H. Kuo, 1999: Typhoons affecting Taiwan: Current understanding and future challenges. *Bull. Amer. Meteor. Soc.,* **80,** 67–80.

——, T.-H. Yen, Y.-H. Kuo, and W. Wang, 2002: Rainfall simulation associated with Typhoon Herb (1996) near Taiwan. Part I: The topographic effect. *Wea. Forecasting,* **17,** 1001–1015.

——, K. K. W. Cheung, and Y.-Y. Lo, 2009: Numerical study of the rainfall event due to interaction of Typhoon Babs (1998) and the northeasterly monsoon. *Mon. Wea. Rev.,* **137,** 2049–2064.

Wu, L., S. A. Braun, J. Halverson, and G. Heymsfield, 2006: A numerical study of Hurricane Erin (2001). Part I: Model verification and storm evolution. *J. Atmos. Sci.,* **63,** 65–86.

——, J. Liang, and C.-C. Wu, 2011a: Monsoonal Influence on Typhoon Morakot (2009). Part I: Observational analysis. *J. Atmos. Sci.,* 2208–2221.

——, H. Zong, and J. Liang, 2011b: Observational analysis of sudden tropical cyclone track changes in the vicinity of the East China Sea. *J. Atmos. Sci.,* in press.

Yang, M.-J., D.-L. Zhang, and H.-L. Huang, 2008: A modeling study of Typhoon Nari (2001) at landfall. Part I: Topographic effects. *J. Atmos. Sci.,* **65,** 3095–3115.

Yeh, T. C., and R. L. Elsberry, 1993a: Interaction of typhoons with the Taiwan orography. Part I: Upstream track deflections. *Mon. Wea. Rev.,* **121,** 3193–3213.

——, and ——, 1993b: Interaction of typhoons with the Taiwan orography. Part II: Continuous and discontinuous tracks across the island. *Mon. Wea. Rev.,* **121,** 3213–3233.